Materials Research. 2018; 21(5): e20171081
DOI: http://dx.doi.org/10.1590/1980-5373-MR-2017-1081

Human Embryonic Stem Cell-Derived Mesenchymal Progenitor (hESCs-MP) Growth on Nanostructured Ti6Al4V Surfaces

***Leonardo Marasca Antonini*[a]*, *Adilar Gonçalves dos Santos Junior*[a], *Gwendolen Reilly*[b], *Célia de Fraga Malfatti*[a]**

[a]*Universidade Federal do Rio Grande do Sul, Av. Bento Gonçalves, 9500, Prédio 43427, Sala 232, 91501-970, Porto Alegre, RS, Brasil*
[b]*Institute for in silico medicine, University of Sheffield, The Pam Liversidge Building, Mappin Street, Sheffield, S1 3JD, United Kingdom*

Received: December 10, 2017; Revised: May 03, 2018; Accepted: July 04, 2018

Nanotexturing processes that focus on enhancing the bone-implant contact, such as electropolishing, have been proposed. The aim of this work was to evaluate the influence of Ti6Al4V surface morphology on human embryonic stem cell-derived mesenchymal progenitor (hESCs-MP) growth. Three surface treatments were used in this study: mechanically polished samples and two types of electropolished samples that were treated for 4 min and 12 min, respectively. The systems were characterized by atomic force microscopy, contact profilometry, X-ray diffraction, and wettability. Each system was submitted to a cell culture containing hESCs-MP cells for 14 days, and the resultant cell growth on each system was then evaluated. The results indicated that surfaces with higher nanometric and micrometric roughnesses experienced greater hESCs-MP cell growth in osteogenic media. The same behavior was not observed for cell growth in non-osteogenic media due to the absence of dexamethasone, which is responsible for controlling protein adsorption on the surface.

Keywords: *hESCs-MP cells, Ti6Al4V, electropolishing, nanometric and micrometric roughness, wettability.*

1. Introduction

Titanium and its alloys have recently been broadly employed as the preferred biomaterial for orthopedic implants due to their desirable mechanical and biological properties[1-3]. It has also been shown that it is important to control the surface properties of these orthopedic implants, such as their corrosion resistance, biocompatibility, mechanical resistance, and fatigue resistance. Ti6Al4V is the most widely used titanium alloy for these applications, as it possesses good mechanical properties, high corrosion resistance, and good biocompatibility[4]. In biomedical applications that aim to enhance the bone-implant osseointegration process, superficial treatment processes and texturing, such as electropolishing and anodization, have been proposed to control surface roughness[5] and wettability[6]. Among the required characteristics of a biomaterial, surface texturing has a strong influence on biocompatibility, adhesion, and cell growth results. Surface texturing treatments thus aim to achieve a better tissue-implant interaction[7].

The use of nanostructured biomaterials in bone regeneration is inspired by the native bone architecture[8], which has also been suggested to further increase the biomimicry and bioactivity of the biomaterials[9]. Many studies have revealed that nanostructured biomaterials promote the process of bone regeneration by supporting cell adhesion, spreading, proliferation, and differentiation[10,11]. Effective interactions between stem cells and nanostructured materials require the design and fabrication of novel biomaterials that can guide the cell behaviors in a desirable way. Stem cells can have strong interactions with nanostructured biomaterials, and nanostructures can guide and enhance the cell function[12].

Zhao et al.[13] reported that nanostructured surfaces of titanium had significant effects on cell differentiation. Furthermore, this nanotopography can stimulate mesenchymal stem cell differentiation in the absence of osteogenic supplements[14-16]. The large surface area and nanostructure of the biomaterial can thus provide more binding sites for the cell receptors, aiding the adsorption and retention of circulating osteogenic factors that contribute to osteogenesis[17,18]. Properties such as nanoscale roughness and nanotopography can induce changes in the cell membrane receptors and activate specific mechanotransduction pathways that direct cell fate in favor of osteogenesis[19,20]. Furthermore, Webster et al.[21] demonstrated that nanostructural modification can accelerate hard-tissue engineering through increased initial cell attachment to the surface.

The topographical properties of the nanostructures on titanium alloy surfaces play important roles in modulating the cell response at the implant-tissue interface, which can have a large effect on tissue integration with the implant[22]. Surfaces with nanostructures possess an increased surface area compared to those without such features[23], with this

*e-mail: leomantonini@gmail.com

increased surface area allowing the increased adhesion of cells, such as osteoblasts and fibroblasts.

Partida et al.[24] studied the effect of TiO_2 nanotubes on Ti6Al4V using super-oxidized water enriched with fluoride, and found that these nanotubes promoted antibacterial activity against Staphylococcus aureus. There was clear evidence that the surface topography of the material influenced bacterial response to the biomaterial, with nanostructured surfaces potentially offering one of the best options to impede infections. Implants with nanostructured surfaces have been widely investigated to determine their capacity to enhance the biocompatibility of orthopedic and dental materials, which may also have improved their antibacterial properties[25].

Marini et al.[26] studied how well the nanostructured surfaces of Ti6Al4V and Ti13Nb13Zr favored the growth and adhesion of human adipose mesenchymal stem cells (hAMSCs) and maintained their osteogenic differentiation. Their results showed that both nanostructured surfaces possessed better osteoconductive properties than surfaces without nanostructures.

Tognarini et al.[27] demonstrated that adipose mesenchymal stem cells (AMSCs) possess the same ability to differentiate into osteoblastic lineages, and to produce the bone matrix of the bone marrow-derived stem cells (BMMSCs). Furthermore, Ti6Al4V with smooth surfaces exhibited an osteoconductive action on AMSCs, granting their differentiation into functional osteoblasts and sustaining bone matrix synthesis and calcification. Gittens et al.[28] showed that the osteogenic properties of nanostructured Ti6Al4V are strongly associated with the different stages of osteogenic differentiation, with human primary osteoblasts able to recognize the nanostructured surface and respond to it with active osteoblast functionality, even in the absence of osteogenic factors within the medium. However, pre-osteoblastic mesenchymal stem cells were not induced into osteoblast differentiation only by the presence of nanostructures.

Many studies have reported the influence of the surface topography on the cell growth and adhesion of cells. Brunette[29] highlighted that the surface texture of an implant has the ability to select certain cell populations and change their functions. Meyle et al.[30] found that both the alignment of the surface topography and the mechanical properties of the cytoskeleton influenced the orientation of the cells. According to Bagno et al.[31], the cell growth on a microstructured substrate exhibited finer extensions, known as filopodia, than the cell growth on smooth substrates. Pfeiffer et al.[32] reported that the patterns of molecule expression and adhesion are shaped by the surface microtopography. It has been found that the cell contacts are predominantly located in the grooves of different topographies, and are not limited to ~10 μm surface structures.

A study by Anselme et al.[33] found the maximum cell number at the lowest (1.2-4.5 μm) and highest (4.5-21 μm) roughnesses. Given the wide range of roughnesses, it was possible to demonstrate that the response of hMSCs to roughness varies with the dimensions of the surface features relative to the cell size (~100 μm). For surface features above and below cell size of the hMSCs, the hMSCs will essentially adhere to the nanoscale and submicron features. When the surface features are approximately the same size as the hMSCs, the curvature of these surface features will lead to a two-fold reduction in the number of attached cells, resulting in minimal adhesion due to the added stress imposed on the cell cytoskeleton. However, Anselme et al.[33] highlighted that if the surfaces can be recorded by atomic force microscopy (AFM; ~20 μm resolution), then there is no discernible correlation between roughness, cell adhesion, and cell size. Adhesion can essentially be governed by the surface roughness and cell size (100 μm), and the cells can be stressed by the deformation imposed on their cytoskeleton from convex and concave surface features.

Studies on electrochemical treatment processes have been undertaken to modify the surface textures of titanium and its alloys[34]. Electrochemical treatment by electropolishing is one case in which the anode oxygen release occurs simultaneously with the removal of the surface material. This exposure of the surface to oxygen can lead to metal passivation, which creates a metal oxide and thus provides improved corrosion resistance[35].

Previous studies have confirmed that surface properties, such as roughness, surface energy, chemical composition, and morphology, influence cellular response. Cell growth, proliferation, and the spreading of osteoblasts on Ti6Al4V samples increases on a smoother surface that possesses a lower roughness. Linez et al.[36] studied Ti6Al4V treated with sandblasting and showed that surfaces with an average roughness (R_a) of 0.62 μm presented spherical cells with few cytoplasmatic prolongations, whereas polished surfaces, with R_a = 0.16 μm, presented flattened osteoblasts with thin cytoplasmic extensions in multiple directions. A study involving human bone marrow osteoblasts on Ti6Al4V, with $R_a = 0.6 \pm 0.2$ μm, showed an increase in cell adhesion and cell proliferation[37]. Zhu et al.[38] observed that the osteoblast growth on titanium surfaces with micrometric roughness presented few cytoplasmic extensions compared to surfaces with submicrometric roughness. Di et al.[39] studied the effect of topography on epithelial cells, and suggested that cell interactions can be related to the microarchitecture of the surfaces.

Based on the knowledge that bone-forming cells are derived from stem cells residing in bone marrow[40], human mesenchymal stem cells (hMSCs) have historically been the main source of cells for bone engineering applications. hMSCs are multipotent stem cells, with the potential to differentiate the mesodermal lineages, including the adipogenic, chondrogenic, and osteogenic lineages, but they can also trans-differentiate toward tissues that are representative of other embryonic germ layers[41].

Mamalis et al.[42] showed that hMSCs were sensitive to titanium surface modifications, and that cell attachment and proliferation were key determinants of biocompatibility, because they dictated cell survival and growth prior to matrix deposition during bone healing. Peri-implant bone formation depends on the ability of stem cells to colonize the implant surface and differentiate into osteoblasts. hMSCs undergo osteoblastic differentiation on microstructured titanium surfaces in the absence of exogenous factors, but the mechanisms are unknown. Olivares-Navarrete et al.[43] indicated that surface properties regulate stem cell fate and induce osteoblast differentiation.

The influence of the surface properties of titanium and its alloys on the behavior of cell growth is well-developed, with most ongoing research focused on the micrometric characteristics of the non-nanostructured surfaces[36,37,44]. This study thus aims to evaluate the effect of nanostructured Ti6Al4V surfaces on the growth of human embryonic stem cell-derived mesenchymal progenitor (hESCs-MP) (Y10090/MPC-301-VIAL, Cellartis®hES-MP 002.5) cell differentiation.

2. Materials and Methods

2.1 Materials

Ti6Al4V was used to evaluate the cell growth of BMMSCs. The samples were approximately 14 mm in diameter and 2 mm thick. The samples were cut from a bar in a CNC lathe Romi C 420. The material was provided by TiBrasil Titânio Ltda., and obtained from the forging process.

The chemical composition of the Ti6Al4V samples was determined by Niton® XL3t GOLDD+ Series x-ray fluorescence (XRF). The results of the analyses are presented in Table 1.

The microstructure of the Ti6Al4V alloy used in this study was analyzed at the Corrosion Research Laboratory-LAPEC at Federal University of Rio Grande do Sul-UFRGS. This analysis was undertaken to capture the cross section microstructure of the Ti6Al4V alloy. The sample was immersed in Kroll's reagent (10 ml HF + 5 ml HNO_3 + 85 ml H_2O), for 15 s, and the microstructure was then evaluated by optical microscopy, using a microscopic OLYMPUS CX31, plan C N, FN22.

The Ti6Al4V microstructure used in this work possessed two metallic phases: α (hexagonal structure) and β (BCC structure; Figure 1), which is expected for this alloy[45]. Phase β (dark region) is predominantly in the grain boundaries, whereas the interiors of the grains, with equiaxial geometry, consist of phase α. Armendia et al.[46] documented the Ti6Al4V microstructure, highlighting that phase α consists of equiaxial geometry and phase β is predominantly on the grain boundaries.

Table 1. Chemical composition of the Ti6Al4V alloy.

Element	(% weight)
V	4.3 ± 0.1
Ti	88.2 ± 0.7
Al	7.4 ± 0.8

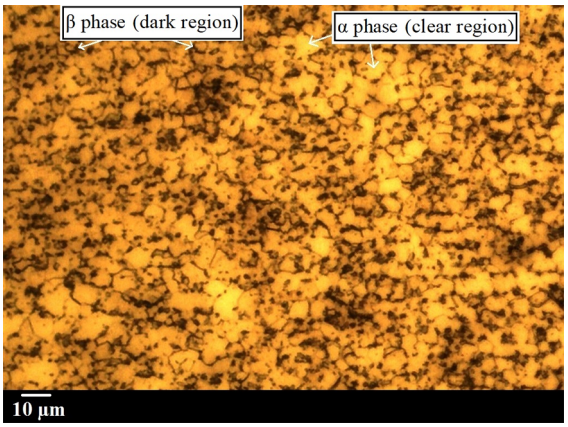

Figure 1. Optical microscopy of the Ti6Al4V cross section.

2.2 Electropolishing procedure

Titanium alloy (Ti6Al4V) disks, with an exposed area of approximately 1.77 cm² and thickness of 2 mm, were used as the substrate. Three systems were used: mechanically polished samples (manually polished) and two types electrochemically treated samples, treated for 4 min and 12 min, respectively. Each sample was first manually polished by abrading the samples with silicon carbide sandpaper (grit size 4000). The samples for electropolishing were washed in water using an ultrasonic bath and dried with cold air. They were then electropolished in an acidic solution consisting of sulfuric acid, hydrofluoric acid, and glycerin in a 6:3:1 (v/v) ratio, using a power source (MPC-303DI, Minipa) that employed platinum as the cathode and the sample as the anode. Electropolishing was carried out for either 4 min or 12 min and 25 V at 7ºC ± 0.5ºC. The choice of electropolishing parameters was based a study by Antonini[47] on titanium surfaces, which showed that longer electropolishing times favor oxide formation, whereas shorter electropolishing times and an electrolyte temperature of ~7ºC favor nanostructured oxide formation. Sulka et al.[48] studied the influence of the anodizing potential on well-ordered nanostructures of aluminum in sulfuric acid, and they observed that an anodizing potential of 25 V resulted in excellent nanopore structures with a regular interpore spacing and pore diameter. After the electrochemical process, the electropolished samples were washed again in an ultrasonic bath for 10 min, with one water change.

2.3 Roughness and wettability analysis

Surface morphology and nanometric roughness were assessed by AFM, using a SHIMADZU SPM-9500J3 microscope, while the micrometric roughness was determined using a GT-K profilometer.

Surface roughness was determined at both the nanometric and micrometric scales by measuring R_a and the vertical distance between the highest peak and the deepest valley within a sample (R_z).

The surface wettability was determined by the sessile drop method, using an apparatus developed by LAPEC/ UFRGS. This made it possible to determine the contact angle between a drop of Dulbecco's Modified Eagle Medium (DMEM; from Sigma-Aldrich Co., LLC) and the analyzed substrate. The contact angle was determined by image analysis, using Surftens 4.5 software.

2.4 Structural characterization of the electropolished samples

The XRD analyses were performed to investigate the presence of oxides on the surface and identify the phases of the samples with known crystalline structures. The analyses were performed with a 2θ of 5º, an applied potential of 40 kV, and a current of 40 mA, using the Philips X-Ray Analytical Equipment X'Pert-MPD System and console PW3040/00 with X-ray tube PW3373/00. The X'Pert High Score software used for the analysis and interpretation of the results.

2.5 Cell culture

hESCs-MPs mesenchymal progenitor cells (Cellartis, Sweden) were used in all of the cell culture experiments. Cells were cultured in gelatin-coated T75 flasks at 37ºC and 5 % CO_2 in basal media (BM), containing Minimum Essential Alpha Medium, 10 % fetal bovine serum, 2 mM L-glutamine, and 100 mg/mL penicillin/streptomycin. During passage, BM was supplemented with 4 ng/mL human fibroblastic growth factor (Life Technologies, UK). Osteogeneis induction media (OIM), consisting of BM supplemented with ascorbic acid (50 µg/mL), beta-glycerolphosphate (5 mM), and dexamethasone (100 nM), were added 24 h after seeding to induce osteoblastic differentiation.

Prior to cell culture, each sample was sterilized by immersion in 70 % ethanol and orbital shaking at 200 rpm for 3 h. After sterilization, the samples were washed three times with Phosphate-buffered saline and orbital shaking at 200 rpm for 20 min for each wash. Samples were seeded at 15,000 cells per sample and a density of 250,000 cells/mL, and then allowed to attach on the surface for 45 min before submerging the disc in 2 mL of BM and incubating them overnight. On day 1, the samples were transferred to a new well plate and 2 mL of OIM was added to selected samples. The media was changed every 2-3 days.

To assess the suitability of the Ti6Al4V samples for cell culture, resazurin reduction (RR) assays were performed. The fluorescence was measured using a microplate reader and was correlated with cell viability[49]. 1 mM Resazurin Sodium Salt in dH_2O was diluted in BM (10 vol %) to create the RR solution. The media was removed from the samples and replaced with 2 ml of RR solution. Well plates were wrapped in foil and incubated for 4 h at 37ºC. 200 µl of the reduced solution was added to a 96-well plate in triplicate and measured using an Infinite F200 Pro Spectrophotometer at λ_{ex} = 540 nm and λ_{em} = 590 nm.

2.6 Statistical analysis

All statistical analyses were undertaken in Graphpad Prism (version 7.00). Three samples were used for each analysis. Depending on whether a response was affected by one or two factors, either a one- or two-way ANOVA with a Tukey's post-test was used to evaluate any significant differences. Differences were considered significant when $*p < 0.05$ and $**p < 0.1$. All graphs are presented as mean ± standard deviation, with notable significant differences indicated on the graphs or in the legends.

3. Results and Discussion

3.1 Structural characterization of the electropolished samples

Figure 2 shows the grazing incidence X-ray diffraction (GIXRD) results at 5º intervals for electropolished samples that were treated for 4 min and 12 min. It was possible to identify the peaks associated with the substrate Ti α (JCPDS file nº. 44-1294) and Ti β (JCPDS file nº. 44-1288).

The GIXRD results showed that it was not possible to identify titanium oxide peaks, regardless of the electrochemical treatment (4 min or 12 min). Although there was oxide formation on the surface, it was not detected, probably due to its minimal thickness. Larsson et al.[50] identified oxide films with thicknesses of <5 nm on electropolished titanium, and recommended the use of either Auger Electron Spectroscopy or XPS analyses to identify these oxides.

According to another work of our research group realized by Antonini et al.[51] it is possible to identified the presence of oxide on the electropolished samples from the XPS analysis, where it was possible to identify oxygen (O1s)

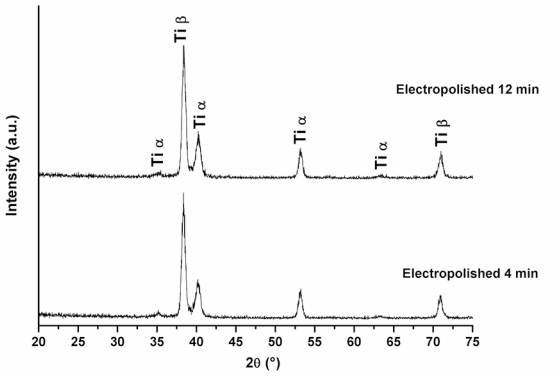

Figure 2. Grazing Incidence X-ray Diffraction (GIXRD) results (incidence angle from 5º) of the electropolished systems, treated for 4 min and 12 min.

on the surface of samples from both of the electropolished systems (4 min and 12 min) at 25 V and 7ºC. This indicates that oxide formation occurred during both electrochemical treatments. The XPS results showed by Antonini et al.[51], in addition to the TiO_2 identified on the electroplated surfaces, evidenced the presence of hydroxide functional groups bound to titanium (TiOH).

3.2 Morphology and wettability

Figure 3 presents the nanometric morphology of the samples obtained by AFM. In Figure 3a is showed an 2D AFM image of the mechanically polished sample, it is possible to observe a surface with irregular morphology; as result of the mechanical preparation. However, the electropolished samples that were treated for 4 min possess a nanostructured surface (Figure 3b), while the electropolished samples that were treated for 12 min possess both, a nanostructured surface and a morphology that is typically associated with oxide formation (Figure 3c). The nanostructures formed because of an anodic dissolution process, which is more intense compared to the oxide formation.

Figure 4 shows the transient of the current density, with a stable transient of the current density observed after 9 min of electrochemical treatment, indicating that the oxide formation on the surface contributes to the decreasing current density as a consequence of the impedance increment. It can thus be seen that the transient of the current density for the samples that were treated for 4 min did not stabilize, whereas the samples that were treated for 12 min maintained a stable transient of the current density for the final 3 min of the electrochemical treatment. Furthermore, it is possible to observe an important anodic dissolution of the electropolished samples that were

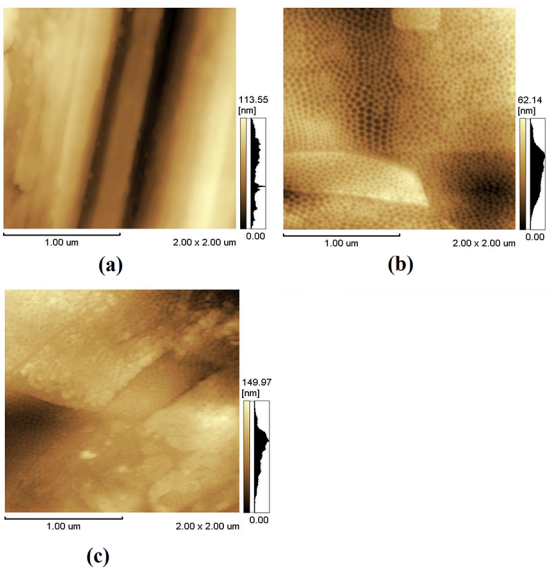

Figure 3. Atomic force microscopic 2D images of the samples used to grow hESCs-MP in non-osteogenic media. (a) Mechanically polished sample; (b) Electropolished sample that was treated for 4 min; and (c) Electropolished sample that was treated for 12 min.

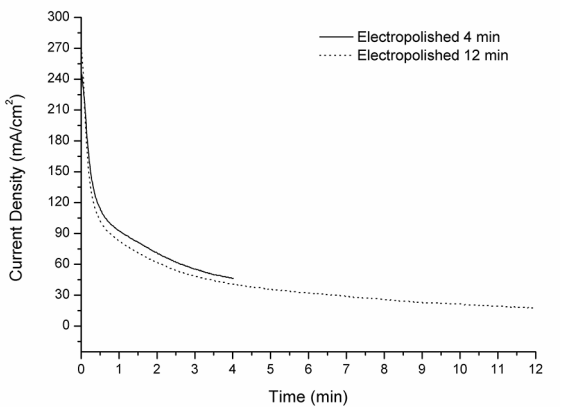

Figure 4. Transients of the current density of the electropolished samples that were treated for 4 min and 12 min.

treated for 4 min (Figure 3b). However, regions of intense oxide formation are observed for the electropolished samples that were treated for 12 min (Figure 3c). The oxide formation may be identified by regions where the nanostructures are not well defined and ordered (i.e., the nanostructures are hidden by the oxide).

Table 2 lists the nanometric and micrometric roughness values of the analyzed samples. From these results, it is evident that the mechanically polished samples (R_a = 24 ± 1 nm) and the electropolished samples that were treated for 12 min (R_a = 18 ± 2 nm) had higher nanometric roughness values than the electropolished samples that were treated for 4 min (R_a = 10 ± 1 nm). The higher R_a values for the electropolished samples that were treated for 12 min can be related to the presence of regions with intense oxide formation (Figure 3c), whereas the R_a values decrease for the electropolished samples that were treated for 4 min due to anodic dissolution. The R_a values of the mechanical polished samples are due to the mechanical sanding. Su et al.[52] conducted a study with nanoporous Ti6Al4V surfaces in contact with rat BMMSCs, and they observed that the best cell growth occurred at R_a = 20 nm, which is similar to the R_a values obtained in this work. Furthermore, Xing et al.[53] and Fujino et al.[54] both demonstrated that a surface roughness between 13 nm and 16 nm was optimal for rat BMMSC cultures, which is closer to the nanometric roughness of the electropolished samples that were treated for 4 min (R_a = 10 ± 1 nm). However, no important differences were observed for the micrometric roughness (R_a) of the studied samples.

The R_z nanometric roughness results for the electropolished samples that were treated for 12 min (R_z = 79 ± 1 nm) provide evidence regarding the effects of dissolution formation and increased oxide layer thickness on the nanometric topography due to the longer electropolishing times. The higher R_z values (R_z = 62 ± 8 nm) for the polished samples may be related to the accentuated difference between the lower and higher regions of the grooves resulting from mechanical polishing. Due to the prevailing thickening of the oxide layer

Table 2. Measurements of nanometric and micrometric roughness.

Systems	Nanometric roughness		Micrometric roughness	
	R_a(nm)	R_z(nm)	R_a(μm)	R_z(μm)
Mechanical polished	24 ± 1	62 ± 8	0.29 ± 0.01	3.74 ± 0.08
Electropolished 4 min	10 ± 1	37 ± 8	0.25± 0.001	3.86 ± 0.07
Electropolished 12 min	18 ± 2	79 ± 1	0.32 ± 0.004	3.99 ± 0.02

on the samples that were electropolished for 12 min, both a greater homogeneity and a smaller difference in relation to dissolution regions are evident, which leads to a lower standard deviation for the R_z values.

Lower R_z values and higher standard deviations for the electropolished samples that were treated for 4 min (R_z = 37 ± 8 nm) were evident, probably due to the greater heterogeneity arising from more intense dissolution in specific regions of the surface during the anodic dissolution process. The highest standard deviations are related to the mechanical polishing process, resulting in reduced control of the nanometric morphology.

There were greater differences in the micrometer roughness values (R_z) between the systems, with higher R_z roughness values for the mechanically polished samples (R_z = 3.74 ± 0.08 μm) and electropolished samples that were treated for 12 min (R_z = 3.99 ± 0.02 μm). For the electropolished samples that were treated for 4 min (R_z = 3.86 ± 0.07 μm), a higher standard deviation was identified, which indicates a greater heterogeneity among the samples compared to the electropolished samples that were treated for 12 min. At micrometric scale, the effect of the anodic dissolution process on micrometric morphology is more pronounced, yielding higher R_z values and associated standard deviations. Higher values were also obtained for the mechanically polished samples, which could be related to the mechanical preparation process, resulting in a more irregular micrometric morphology.

The wettability results highlight lower contact angles in DMEM for the electropolished samples that were treated for 4 min (55° ± 1) compared to the electropolished samples that were treated for 12 min (82° ± 1) and the mechanical polished samples (85° ± 1). The surface wettability is likely influenced by the surface roughness. The samples that were electropolished for 4 min possessed nanostructured surfaces and lower nanometric roughness values, which likely contributed to the observed decrease in contact angle, and thus promoted a hydrophilic behavior. These inferences are supported by the work of Kim et al.[55], who also obtained lower water contact angle values on the nanostructured titanium surface.

Gittens et al.[56] showed that Ti surface modification can improve its hydrophilic properties by changing the surface chemistry, but this present work highlights that surface roughness plays an important role in regulating the degree of surface wettability. Coutinho[57] studied the influence of superficial treatments on titanium, and observed that anodized titanium possessed lower roughnesses and smaller contact angles than polished titanium surfaces. Komasa et al.[58] demonstrated that titania (titanium oxide) nanosheet-modified titanium alloys were more hydrophilic and exhibited markedly improved wettabilities compared to unmodified titanium alloys.

Furthermore, the more hydrophilic behavior of the electropolished samples that were treated for 4 min may have been influenced by the presence of OH functional groups and CF_3 groups, which were also found in the study conducted by Antonini et al.[51]. The electropolished samples that were treated for 4 min adsorbed these groups, which are able to make bridges of H with water, resulting in increased interactions between this surface and the aqueous medium. The wettability of this surface is thus greater than the surfaces that were electropolished for 12 min and mechanically polished. These surface nanostructures may also promote interactions involving electrostatic and van der Waals forces, resulting in a higher affinity of the surface with the initial coating (e.g., fibronectin or vinculin) formed by different proteins that must be synthesized and deposited over a surface for proper cellular growth and proliferation[59,60].

3.3 Evaluation of the growth of human embryonic stem cell-derived mesenchymal progenitor (hESCs-MP) cells in osteogenic media (OIM) and in non-osteogenic media (SM)

Figure 5 highlights the cell growth in osteogenic media (with dexamethasone addition), where the average number of cells was similar for all systems evaluated between day 1 and day 7. However, on day 14 the mechanical polished samples and the electropolished samples that were treated for 12 min possessed more cell growth than the electropolished samples that were treated for 4 min. The micrometric roughness values for all the systems evaluated (mechanically polished and electropolished samples) were on the order of 0.3 μm. These

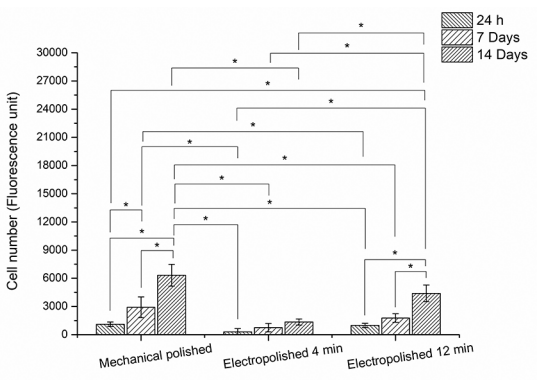

Figure 5. Average number of cells per sample after cell growth in osteogenic media. *p < 0.05.

values were similar to those found by Webster and Ejiofor[21], which observed that low values of micrometric roughness promoted an increase in cellular adhesion on titanium (0.5-2.4 µm), Ti6Al4V (0.5-1.4 µm), and Co28Cr6Mo alloy (0.2-0.4 µm) samples. However, the mechanically polished samples and the electropolished samples that were treated for 12 min possessed high nanometric roughness (R_a and R_z) values, which may have contributed to the increased cell growth observed on day 14.

These observations are in agreement with Andersson et al.[61], where they demonstrated that the increase in nanometric roughness favored the alignment of the cells and subsequent release of cytokines. Furthermore, Wan et al.[62] showed that osteoprogenitor cells exhibited an increase in cellular adhesion on the surfaces with greater nanometric roughness when compared to smoother surfaces that possessed smaller nanometric roughness.

Rex et al.[63] have also shown that cell adhesion appears be more strongly influenced by a rougher surface. Their study indicated that the nanometric roughness would alter the surface properties, as well as influence cell morphology, adhesion strength, and proliferation.

Considering the results obtained in the present work, it is possible to evidence that the increase in nanometric roughness had a more significant effect than wettability on cell growth in osteogenic media. However, cell attachment and growth are complex processes that involves several surface features, including topographic morphology, surface roughness, surface chemistry, and phase state, extending well beyond the realm of surface nanostructures[47,64].

The average number of cells, which was similar for all the systems evaluated between day 1 and day 14, is presented on Figure 6, Even though the systems possessed different nanometric roughness (R_a and R_z) values (Table 2) and wettability results, these parameters did not affect cell growth in the non-osteogenic media, and all the systems showed similar cell growth.

Based on the knowledge that dexamethasone controls and even inhibits the synthesis of proteins[65], the formation and subsequent adhesion of proteins on the surface of the biomaterial is larger during cell growth in the non-osteogenic medium (without dexamethasone). As indicated by Singh et al.[66], surfaces with a high adhesion of proteins can promote the formation of a thick layer of proteins, which then acts a barrier layer that smooths the surface on the nanometer scale.

The formation of this protein barrier layer on the surface of the samples in contact with the non-osteogenic medium favored surface leveling. This protein barrier layer countered the effects of nanometric roughness and wettability in contact with hESCs-MP cells, yielding similar levels of reduced cellular growth (Figure 6).

Reduced cell growth was observed in the osteogenic media (Figure 5) compared to the non-osteogenic media (Figure 6). This observed behavior is in agreement with Rosa et al.[67] study, which detected reduced cell growth in a culture media containing dexamethasone compared to a culture media without this substance.

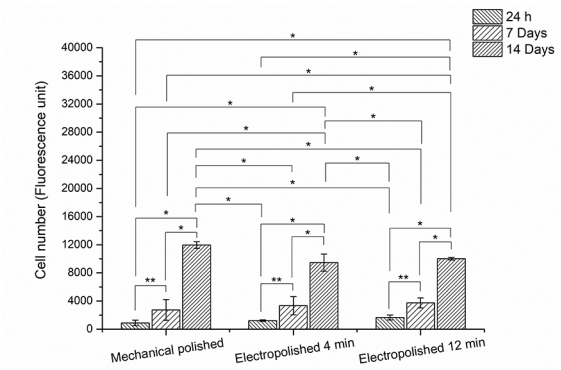

Figure 6. Average number of cells per sample after cell growth in non-osteogenic media. *p < 0.05, **p < 0.1.

4. Conclusion

The samples that were electropolished for 4 min developed surface nanostructures, while the samples that were electropolished samples for 12 min developed surface nanostructures and an oxide layer.

The mechanically polished samples and the electropolished samples that were treated for 12 min possessed higher nanometric roughnesses than the electropolished samples that were treated for 4 min. However, no notable micrometric roughness differences were observed. Furthermore, in this work it was verified that increasing the nanometric roughness had a more significant effect than wettability on the cell growth in osteogenic media.

The effects of nanometric roughness, micrometric roughness, and surface chemical composition on cellular growth in non-osteogenic media were not observed in this study. However, hESCs-MP cell growth in an osteogenic medium increases as the nanometric roughness increases. These behaviors indicate that the presence of dexamethasone in the osteogenic medium controls the growth of protein, avoiding the formation of a protein barrier. This protein barrier minimizes the effect of nanometric morphology on cell growth, as it was observed for cellular growth in non-osteogenic media.

5. Acknowledgments

This present work was carried out with the support of CAPES and CNPq, Brazilian Government entities focused on human resources formation. We thank Julie Marshall, University of Sheffield, for technical services relating to the cell culture work.

6. References

1. Niinomi M. Mechanical biocompatibilities of titanium alloys for biomedical applications. *Journal of the Mechanical Behavior of Biomedical Materials*. 2008;1(1):30-42.

2. Ryan GE, Pandit AS, Apatsidis DP. Porous titanium scaffolds fabricated using a rapid prototyping and powder metallurgy technique. *Biomaterials*. 2008;29(27):3625-3635.

3. Khosroshahi ME, Mahmoodi M, Saeedinasab H, Tahriri M. Evaluation of mechanical and electrochemical properties of laser surface modified Ti-6Al-4V for biomedical applications: in vitro study. *Surface Engineering*. 2008;24(3):209-218.

4. Huang CA, Hsu F, Yu CH. Electropolishing behavior of pure titanium in sulfuric acid-ethanol electrolytes with an addition of water. *Corrosion Science*. 2011;53(2):589-596.

5. Lopes NIA, Silva LAO, Santos LA, Buono VLT. Surface Characterization of NiTi Superelastic and Shape Memory Alloys After Electrolytic Polishing. *Materials Research*. 2017;20(Suppl 2):572-579.

6. Escada AL, Nakazato RZ, Claro APRA. Influence of Anodization Parameters in the TiO_2 Nanotubes Formation on Ti-7.5Mo Alloy Surface for Biomedical Application. *Materials Research*. 2017;20(5):1282-1290.

7. Klymov A, Bronkhorst EM, te Riet J, Jansen JA, Walboomers XF. Bone marrow-derived mesenchymal cells feature selective migration behavior on submicro- and nano-dimensional multi-patterned substrates. *Acta Biomaterialia*. 2015;16:117-125.

8. Landis WJ, Silver FH. Mineral deposition in the extracellular matrices of vertebrate tissues: identification of possible apatite nucleation sites on type I collagen. *Cells, Tissues, Organs*. 2009;189(1-4):20-24.

9. Tomsia AP, Lee JS, Wegst UG, Saiz E. Nanotechnology for dental implants. *International Journal of Oral & Maxillofacial Implants*. 2013;28(6):e535-e546.

10. Martínez E, Engel E, Planell JA, Samitier J. Effects of artificial micro-and nano-structured surfaces on cell behaviour. *Annals of Anatomy*. 2009;191(1):126-135.

11. Lord MS, Foss M, Besenbacher F. Influence of nanoscale surface topography on protein adsorption and cellular response. *Nanotoday*. 2010;5(1):66-78.

12. Wang P, Zhao L, Liu J, Weir MD, Zhou X, Xu HH. Bone tissue engineering via nanostructured calcium phosphate biomaterials and stem cells. *Bone Research*. 2014;2:14017.

13. Zhao L, Liu L, Wu Z, Zhang Y, Chu PK. Effects of micropitted/nanotubular titania topographies on bone mesenchymal stem cell osteogenic differentiation. *Biomaterials*. 2012;33(9):2629-2641.

14. Liao S, Nguyen LT, Ngiam M, Wang C, Cheng Z, Chan CK, et al. Biomimetic nanocomposites to control osteogenic differentiation of human mesenchymal stem cells. *Advanced Healthcare Materials*. 2014;3(5):737-751.

15. Lock J, Liu H. Nanomaterials enhance osteogenic differentiation of human mesenchymal stem cells similar to a short peptide of BMP-7. *International Journal of Nanomedicine*. 2011;6:2769-2777.

16. Polini A, Pisignano D, Parodi M, Quarto R, Scaglione S. Osteoinduction of human mesenchymal stem cells by bioactive composite scaffolds without supplemental osteogenic growth factors. *PLoS One*. 2011;6(10):e26211.

17. Koegler P, Clayton A, Thissen H, Santos GN, Kingshott P. The influence of nanostructured materials on biointerfacial interactions. *Advanced Drug Delivery Reviews*. 2012;64(15):1820-1839.

18. Fricain JC, Schlaubitz S, Le Visage C, Arnault I, Derkaoui SM, Siadous R, et al. A nano-hydroxyapatite-pullulan/dextran polysaccharide composite macroporous material for bone tissue engineering. *Biomaterials*. 2013;34(12):2947-2959.

19. Nikukar H, Reid S, Tsimbouri PM, Riehle MO, Curtis AS, Dalby MJ. Osteogenesis of mesenchymal stem cells by nanoscale mechanotransduction. *ACS Nano*. 2013;7(3):2758-2767.

20. Mendonça G, Mendonça DB, Simões LG, Araújo AL, Leite ER, Duarte WR, et al. The effects of implant surface nanoscale features on osteoblast-specific gene expression. *Biomaterials*. 2009;30(25):4053-4062.

21. Webster TJ, Ejiofor JU. Increased osteoblast adhesion on nanophase metals: Ti, Ti6Al4V, and CoCrMo. *Biomaterials*. 2004;25(19):4731-4739.

22. Boyan BD, Bonewald LF, Paschalis EP, Lohmann CH, Rosser J, Cochran DL, et al. Osteoblast mediated mineral deposition in culture is dependent on surface microtopography. *Calcified Tissue International*. 2002;71(6):519-529.

23. Mendonça G, Mendonça DB, Aragão FJ, Cooper LF. The combination of micron and nanotopography by H_2SO_4/H_2O_2 treatment and its effects on osteoblast-specific gene expression of hMSCs. *Journal of Biomedical Materials Research: Part A*. 2010;94(1):169-179.

24. Beltrán-Partida E, Valdez-Salas B, Escamilla A, Moreno-Ulloa A, Burtseva L, Valdez-Salas E, et al. The Promotion of Antibacterial Effects of Ti6Al4V Alloy Modified with TiO2 Nanotubes Using a Superoxidized Solution. *Journal of Nanomaterials*. 2015;2015:818565.

25. Wang F, Shi L, He WX, Han D, Yan Y, Niu ZY, et al. Bioinspired micro/nano fabrication on dental implant-bone interface. *Applied Surface Science*. 2013;265:480-488.

26. Marini F, Luzi E, Fabbri S, Ciuffi S, Sorace S, Tognarini I, et al. Osteogenic differentiation of adipose tissue-derived mesenchymal stem cells on nanostructured Ti6Al4V and Ti13Nb13Zr. *Clinical Cases in Mineral and Bone Metabolism*. 2015;12(3):224-237.

27. Tognarini I, Sorace S, Zonefrati R, Galli G, Gozzini A, Carbonell Sala S, et al. In vitro differentiation of human mesenchymal stem cells on Ti6Al4V surfaces. *Biomaterials*. 2008;29(7):809-824.

28. Gittens RA, Olivares-Navarrete R, McLachlan T, Cai Y, Hyzy SL, Schneider JM, et al. Differential responses of osteoblast lineage cells to nanotopographically-modified, microroughned titanium-aluminum-vanadium alloy surfaces. *Biomaterials*. 2012;33(35):8986-8994.

29. Brunette DM. The effects of implant surface topography on the behavior of cells. *International Journal of Oral & Maxillofacial Implants*. 1988;3(4):231-246.

30. Meyle J, Gültig K, Wolburg H, von Recum AF. Fibroblast anchorage to microtextured surfaces. *Journal of Biomedical Materials Research*. 1993;27(12):1553-1557.

31. Bagno A, Di Bello C. Surface treatments and roughness properties of Ti-based biomaterials. *Journal of Materials Science: Materials in Medicine*. 2004;15(9):935-949.

32. Pfeiffer, F, Herzog B, Kern D, Scheideler L, Geis-Gerstorfer J, Wolburg H. Cell reactions to microstructured implant surfaces. Microelectronic Engineering. 2003;67-68:913-922.

33. Anselme K, Bigerelle M. On the relation between surface roughness of metallic substrates and adhesion of human primary bone cells. *Scanning*. 2014;36(1):11-20.

34. Carvalho DR, Carvalho PS, Magro Filho O, de Mello JD, Beloti MM, Rosa AL. Characterization and in vitro cytocompatibility of an acid-etched-titanium surface. *Brazilian Dental Journal*. 2010;21(1):3-11.

35. Yang G, Wang B, Tawfiq K, Wei H, Zhou S, Chen G. Electropolishing of surfaces: theory and applications. *Surface Engineering*. 2017;33(2):149-166.

36. Linez-Bataillon P, Monchau F, Bigerelle M, Hildebrand HF. In vitro MC3T3 osteoblast adhesion with respect to surface roughness of Ti6Al4V substrates. *Biomolecular Engineering*. 2002;19(2-6):133-141.

37. Deligianni DD, Katsala N, Ladas S, Sotiropoulou D, Amedee J, Missirlis YF. Effect of surface roughness of the titanium alloy Ti-6A1-4V on human bone marrow cell response and on protein adsorption. *Biomaterials*. 2001;22(11):1241-1251.

38. Zhu X, Chen J, Scheideler L, Altebaeumer T, Geis-Gerstorfer J, Kern D. Cellular reactions of osteoblasts to micron- and submicron-scale porous structures of titanium surfaces. *Cells, Tissues, Organs*. 2004;178(1):13-22.

39. Di Carmine M, Toto P, Feliciani C, Scarano A, Tulli A, Strocchi R, et al. Spreading of epithelial cells on machined and sandblasted titanium surfaces: an in vitro study. *Journal of Periodontolology*. 2003;74(3):289-295.

40. Bab I, Passi-Even L, Gazit D, Sekeles E, Ashton BA, Peylan-Ramu N, et al. Osteogenesis in in vivo diffusion chamber cultures of human marrow cells. *Bone and Mineral*. 1988;4(4):373-386.

41. Pittenger MF, Mackay AM, Beck SC, Jaiswal RK, Douglas R, Mosca JD, et al. Multilineage potential of adult human mesenchymal stem cells. *Science*. 1999;284(5411):143-147.

42. Mamalis A, Silvestros S. Modified titanium surfaces alter osteogenic differentiation: a comparative microarray-based analysis of human mesenchymal cell response to commercial titanium surfaces. *Journal of Oral Implantology*. 2013;39(5):591-601.

43. Olivares-Navarrete R, Hyzy SL, Park JH, Dunn GR, Haithcock D, Wasilewski C, et al. Mediation of osteogenic differentiation of human mesenchymal stem cells on titanium surfaces by a Wnt-integrin feedback loop. *Biomaterials*. 2011;32(27):6399-6411.

44. Kuhn A. The electropolishing of titanium and its alloys. *Metal Finishing*. 2004;102(6):80-86.

45. Hkrawiec H, Vignal V, Schwarzenboeck E, Banas J. Role of plastic deformation and microstructure in the micro-electrochemical behaviour of Ti-6Al-4V in sodium chloride solution. *Electrochimica Acta*. 2013;104:400-406.

46. Armendia M, Garay A, Iriarte LM, Arrazola PJ. Comparison of the machinabilities of Ti6Al4V and TIMETAL(r) 54M using uncoated WC-Co tools. *Journal of Materials Processing Technology*. 2010;210(2):197-203.

47. Antonini LM. *Superfícies nanoestruturais de titânio e tratamento superficial com filmes Diamond Like Carbon (DLC)*. [Dissertation]. Porto Alegre: Universidade Federal do Rio Grande do Sul; 2012.

48. Sulka GD, Parkola KG. Anodising potential influence on well-ordered nanostructures formed by anodisation of aluminium in sulphuric acid. *Thin Solid Films*. 2006;515(1):338-345.

49. O'Brien J, Wilson I, Orton T, Pognan F. Investigation of the Alamar Blue (resazurin) fluorescent dye for the assessment of mammalian cell cytotoxicity. *European Journal of Biochemistry*. 2000;267(17):5421-5426.

50. Larsson C, Thomsen P, Aronsson BO, Rodahl M, Lausmaa A, Kasemo B, et al. Bone response to surface-modified titanium implants: studies on the early tissue response to machined and electropolished implants with different oxide thicknesses. *Biomaterials*. 1996;17(6):605-616.

51. Antonini LM, Kothe V, Reilly GC, Owen R, Marcuzzo JS, Malfatti CF. Effect of the Ti6Al4V surface morphology on the osteogenic differentiation of human embryonic stem cells. *Journal of Materials Research*. 2017;32(20):3811-3821.

52. Su Y, Komasa S, Sekino T, Nishizaki H, Okazaki J. Characterization and Bone Differentiation of Nanoporous Structure Fabricated on Ti6Al4V Alloy. *Journal of Nanomaterials*. 2015;2015:358951.

53. Xing H, Komasa S, Taguchi Y, Sekino T, Okazaki J. Osteogenic activity of titanium surfaces with nanonetwork structures. *International Journal of Nanomedicine*. 2014;9:1741-1755.

54. Fujino T, Taguchi Y, Komasa S, Sekino T, Tanaka M. Cell Differentiation on Nanoscale Features of a Titanium Surface: Effects of Deposition Time in NaOH Solution. *Journal of Hard Tissue Biology*. 2014;23(1):63-70.

55. Kim HS, Kim YJ, Jang JH, Park JW. Surface Engineering of Nanostructured Titanium Implants with Bioactive Ions. *Journal of Dental Research*. 2016;95(5):558-565.

56. Gittens RA, Scheideler L, Rupp F, Hyzy SL, Gerstorfer JG, Schwartz Z, et al. A review on the wettability of dental implant surfaces II: Biological and clinical aspects. *Acta Biomaterialia*. 2014;10(7):2907-2918.

57. Coutinho MP. *Influência da morfologia e da superfície na molhabilidade do titânio comercialmente puro*. [Dissertation]. Rio de Janeiro: Instituto Militar de Engenharia; 2007.

58. Komasa S, Kusumoto T, Taguchi Y, Nishizaki H, Sekino T, Umeda M, et al. Effect of Nanosheet Surface Structure of Titanium Alloys on Cell Differentiation. *Journal of Nanomaterials*. 2014;2014:642527.

59. Kopf BS, Ruch S, Berner S, Spencer ND, Maniura-Weber K. The role of nanostructures and hydrophilicity in osseointegration: in-vitro protein-adsorption and blood-interaction studies. *Journal*

of Biomedical Materials Research: Part A. 2015;103(8):2661-2672.

60. Puleo DA, Nanci A. Understanding and controlling the bone-implant interface. *Biomaterials*. 1999;20(23-24):2311-2321.

61. Andersson AS, Bäckhed F, von Euler A, Richter-Dahlfors A, Sutherland D, Kasemo B. Nanoscale features influence epithelial cell morphology and cytokine production. *Biomaterials*. 2003;24(20):3427-3436.

62. Wan Y, Wang Y, Liu Z, Qu X, Han B, Bei J, et al. Adhesion and proliferation of OCT-1 osteoblast-like cells on micro- and nano-scale topography structured poly(L-lactide). *Biomaterials*. 2005;26(21):4453-4459.

63. Wang RC, Hsieh MC, Lee TM. Effects of nanometric roughness on surface properties and fibroblast's initial cytocompatibilities of Ti6Al4V. *Biointerphases*. 2011;6(3):87.

64. Silva WM, Ribeiro CA, Marques CS, Tabata AS, Saeki MJ, Medeiros LI, et al. Fibroblast and pre-osteoblast cell adhesive behavior on titanium alloy coated with diamond film. *Materials Research*. 2017;20(Suppl 2):284-290.

65. Huang DP, Schwartz CE, Chiu JF, Cook JR. Dexamethasone Inhibition of Rat Hepatoma Growth and a-Fetoprotein Synthesis. *Cancer Research*. 1984;44(7):2976-2980.

66. Singh AV, Vyas V, Patil R, Sharma V, Scopelliti PE, Bongiorno G, et al. Quantitative characterization of the influence of the nanoscale morphology of nanostructured surfaces on bacterial adhesion and biofilm formation. *PLoS One*. 2011;6(9):e25029.

67. Beloti MM, Rosa AL. Osteoblast differentiation of human bone marrow cells under continuous and discontinuous treatment with dexamethasone. *Brazilian Dental Journal*. 2005;16(2):156-161.